LOSSES ON SPS FLAT BOTTOM AND BEAM LOADING WITH LHC BEAMS

H. Bartosik*, T. Bohl, S. Cettour Cave, K. Cornelis, H. Damerau, B. Goddard,V. Kain, A. Lasheen, G. Rumolo, E. Shaposhnikova, H. Timko, CERN, Geneva

Abstract

Losses at SPS flat bottom with the LHC proton beams had been studied since the earliest days the LHC beams became available in the SPS. Some of the loss mechanisms involved could be identified and over the years of operation with the nominal 25 ns LHC beam, the losses could be gradually reduced. Nevertheless, in machine studies with high intensity 25 ns LHC beams it is still observed that the transmission degrades with intensity. As summarised in this paper, a series of studies have been performed in 2016 with the aim of further characterising the loss mechanisms and eventually finding mitigation measures in view of the LHC injector upgrade project (LIU).

INTRODUCTION

Losses at SPS flat bottom with the LHC proton beams had been studied since the earliest days the LHC beams became available in the SPS. The conclusions of four reports are summarized below to illustrate the understanding of the losses at certain times.

Historical context

2000 In 2000 the following was reported [1]: A total intensity of 1×10^{13} in three batches was accelerated to top energy with a transmission efficiency of 70%. Continuous particle losses are observed on the flat bottom for high intensities. The reason is not clear. The high intensity beam is unstable on the flat top independent of the final voltage value, however the situation seems to be worse for lower voltage. Limitations to the intensity are a) too large a longitudinal emittance sent by the PS for intensities above 3×10^{12} per batch, b) the acceptance of the SPS in connection with this large injected emittance and c) possibly noise in RF loops (causing additional emittance blow-up).

2004 In 2004 the following was reported [2]: While nominal LHC beams have been accelerated in the SPS, transmission loss is important for future intensity increases. Capture losses are due to a combination of injected bunch length, injection errors and bucket size reduction due to energy loss. The losses along the injection plateau are not fully understood. The effect of coherent lines in the presence of white noise, the effect of the transverse working point, and the influence of low-amplitude instabilities on parts of the batch have been seen but do not explain the whole picture. In addition the possible presence of ions could have an effect, which should be studied. Similar effects in the LHC itself could have serious consequences, the injection plateau at 450 GeV/c being 20 min long with no synchrotron radiation damping, which conversely will have a significant effect at 7 TeV.

2006 The following was reported at the LHC Machine Advisory Committee [3] in December 2006: A reduction of the low energy losses from >10 to 7-8% was achieved by a) a new RF voltage programme (end of 2003) and b) a new working point compatible with larger momentum spread (end of 2004) and large vertical chromaticity required to fight the ECI (see Fig. 1). Short lifetime on the injection plateau was observed even after optimization of the working point. The longitudinal lifetime dominates (capture losses due to real part of the longitudinal impedance and the bunch shape), which should be improved by impedance reduction and optimization of the bunch shape from PS. The difference in lifetime between the head and the tail of the batch recovers as the intensity decreases: Bunches are getting shorter particularly at the tail of the batch ... while the electron cloud signal disappears. Need to understand better the blow-up and loss mechanisms at the beginning of the ramp (mainly on the tail of the 4th batch).

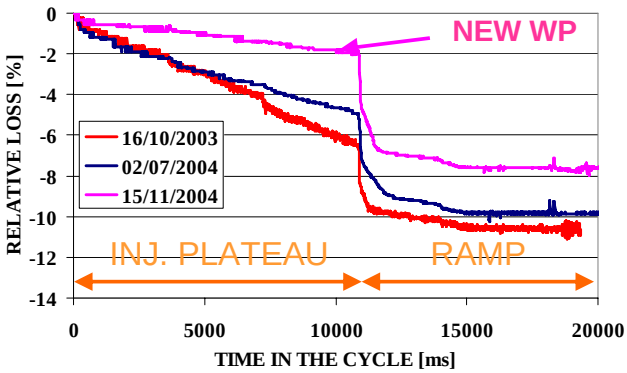

Figure 1: Losses for different working points, taken from [3].

2012 In 2012 the following was reported [4]: Detailed simulations of the PS-to-SPS longitudinal beam transfer determined the main longitudinal beam loss mechanism in the SPS. The simulated longitudinal phase-space distribution of a typical bunch after the PS rotation, at injection into the SPS bucket is shown in Fig. 2. The simulations demonstrated that using the minimum bunch length at PS-to-SPS transfer as a criterion for best transmission is not necessarily appropriate; instead, the phase-space bunch distribution should be optimised as a function of the bunch rotation timings used in the PS. Systematic measurements with 36 bunches of LHC-type

* hannes.bartosik@cern.ch

https://doi.org/10.23727/CERN-Proceedings-2017-002.63

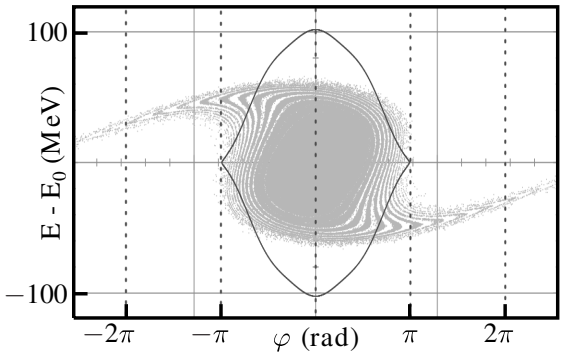

Figure 2: Simulated particle phase-space distribution at injection into the SPS bucket (V_{200} MHz = 2 MV and V_{800} MHz = 0.34 MV in bunch-shortening mode) under operational conditions [4].

50 ns beam in a short cycle gave reproducible, consistent results. The predicted optimal timings and the qualitative transmission and bunch length behaviour obtained from simulations is in excellent agreement with experimental results. With the spare 40 MHz cavity, a significant loss reduction of about 50% can be achieved with bunches that are shorter than operational. Alternatively, the longitudinal emittance can be increased by 40% while keeping the operational transmission, which allows for a stable beam in the PS even at significantly higher intensities. To better estimate the transmission and emittance requirements at the ultimate intensity required by the high luminosity LHC, simulations including impedance effects are underway. Due to the recent failure of a 40 MHz cavity in the PS, the new bunch rotation settings could not yet be tested under operational conditions, but they shall be tested as soon as it will be possible.

Studies in view of the LHC injector upgrade

The LHC injector upgrade project (LIU) [5] aims at consolidating and upgrading the existing injector chain at CERN in view of the beam parameters required for the High Luminosity LHC (HL-LHC) era. The aim is to provide 2.3×10^{11} p/b at LHC injection with about twice the brightness compared to today's operation. To reach these parameters, an extensive upgrade of the SPS RF system during Long Shutdown 2 will resolve intensity limitations from insufficient beam loading compensation. The LIU parameters require ≤10% losses from PS extraction to SPS extraction.

Electron cloud is one of the issues encountered especially in the early years of operation with 25 ns beams. Although some conditioning of the machine has been achieved through scrubbing runs and machine operation over the years, it is still not fully clear if the e-cloud effect will pose a limitation on the beam performance in the HL-LHC era. In the last years extensive studies have been performed in the frame of the LIU project. The last high intensity scrubbing run was performed in 2015. During that period the Q20 optics [6] (implemented and operational for LHC beams since 2012 to mitigate transverse single bunch transverse instabilities at injection) was used. With 4 batches of the 25 ns LHC beam and 2×10^{11} p/b the losses on the flat bottom alone already exceeded the target of 10%. As discussed in what follows, a series of measurements where therefore performed in 2016 in order to further investigate the loss mechanisms involved. Also the open question of the contribution from e-cloud effects was addressed.

STUDIES OF LOSSES IN THE SPS IN 2016

The machine studies in 2016 concentrated on 25 ns beams on a special MD cycle, which has a 7.8 s long injection plateau at 26 GeV/c and a 7.8 s long intermediate plateau at 28 GeV/c. This allowed distinguishing losses due to uncaptured beam on the injection plateau from other losses when storing the beam at almost the same energy. All studies presented here were performed with the Q20 optics.

Losses as a function of longitudinal emittance

The dependence of the losses on the longitudinal emittance at PS extraction was studied for a single batch of a low intensity LHC25ns (standard) beam, i.e. with 72 bunches of about 6.9×10^{10} p/b injected, which is about half of the nominal intensity. This allowed reaching very low longitudinal emittances without rendering the beam unstable in the PS. The longitudinal emittance can then be varied with controlled blow-up along the PS ramp. The SPS cycle was programmed for a calculated bucket area of about 0.6 eVs as used in routine operation. The voltage on the 800 MHz RF was set to 1/10 of the voltage at 200 MHz and the phase set to bunch shortening mode.

Figure 3 summarizes the results of the measurements: The plot on the left shows the BCT intensities averaged for the different longitudinal emittance cases along the cycle and on the right plot the relative losses on the flat bottom are compared to the relative losses from injection up to the beginning of the 28 GeV/c plateau (i.e. including the losses during the first ramp). Losses of about 1% are observed for the smallest longitudinal emittance, i.e. 0.2 eVs. The transmission degrades with larger longitudinal emittance, since the large longitudinal tails resulting from the bunch rotation at PS extraction cannot be captured in the SPS RF bucket. Therefore the losses occur mainly during the ramp. It is interesting to note however that there are also some losses on the flat portions of the cycle. Furthermore losses are observed also on the second ramp. These losses also increase with the longitudinal emittance as the RF bucket becomes very full.

Losses as a function of SPS bucket area

Losses in the SPS as a function of the bucket area were studied using a BCMS beam with 48 bunches and 1.3×10^{11} p/b. The beam had a bunch length of 4 ns at injection corresponding to the canonical longitudinal emittance of 0.35 eVs. Figure 4 shows the resulting losses with the 800 MHz OFF and with the 800 MHz ON (voltage ratio

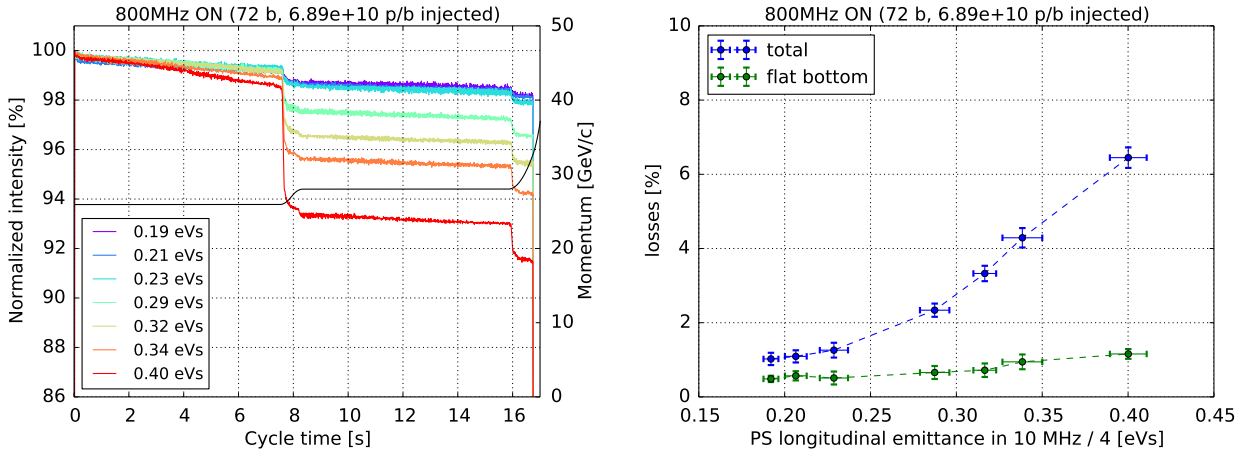

Figure 3: Losses as a function of longitudinal emittance as measured in the PS before bunch rotation. Left: Averaged BCT signal for different longitudinal emittances. Right: Relative losses on flat bottom compared to the relative losses from injection up to the beginning of the 28 GeV/c plateau.

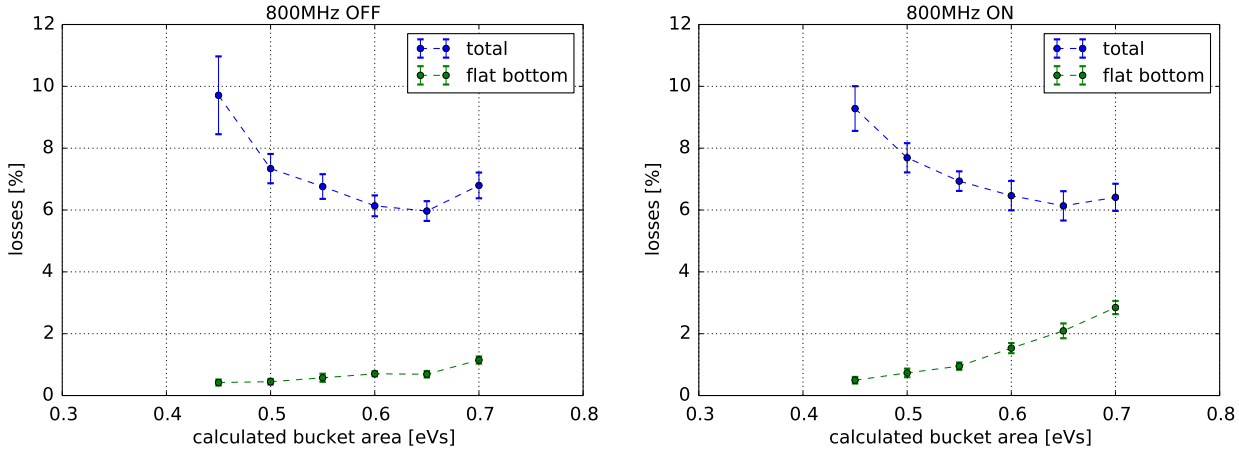

Figure 4: Losses on the flat bottom and total losses up to the beginning of the 28 GeV/c intermediate plateau as a function of the bucket area in the SPS for the case with 800 MHz RF system OFF (left) and ON (right) as described in the text.

1/10 with respect to the 200 MHz voltage, bunch shortening mode). With 800 MHz OFF the losses on the flat bottom show a slight but monotonic increase with larger bucket area (i.e. larger voltage), while the total losses including the ramp to 28 GeV/c show a minimum at the operational setting of 0.65 eVs: For smaller bucket areas the capture losses dominate; for larger bucket area the losses are also higher, most likely because particles in the bucket start reaching the momentum aperture limitation with the large dispersion in the Q20 optics. In the case with 800 MHz ON the total losses show a very similar behaviour, however the flat bottom losses in this case significantly increase as a function of the bucket area. In other words, in the case with the 800 MHz ON the flat bottom losses are enhanced without affecting the total losses. This was further investigated as described below.

Effect of 800 MHz RF on losses

To distinguish losses due to uncaptured beam from losses due to particles inside the RF buckets, the SPS vertical tune

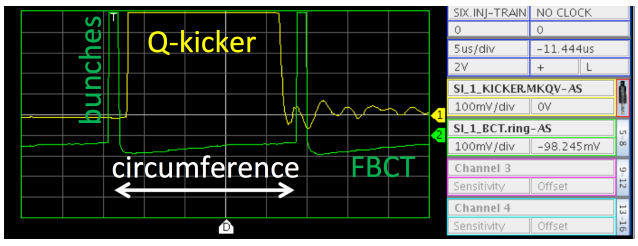

Figure 5: Adjustment of MKQV kicker waveform to clean uncaptured beam.

kicker MKQV was used at full kick strength to clean the part of the SPS circumference without bunches. To this end, the waveform of the kicker was carefully adjusted to pulse in a single turn in between the passage of the bunch train as illustrated in Fig. 5. Such a kick with the MKQV can be applied once per cycle. Figure 6 shows the intensity evolution with 800 MHz RF OFF compared to the case

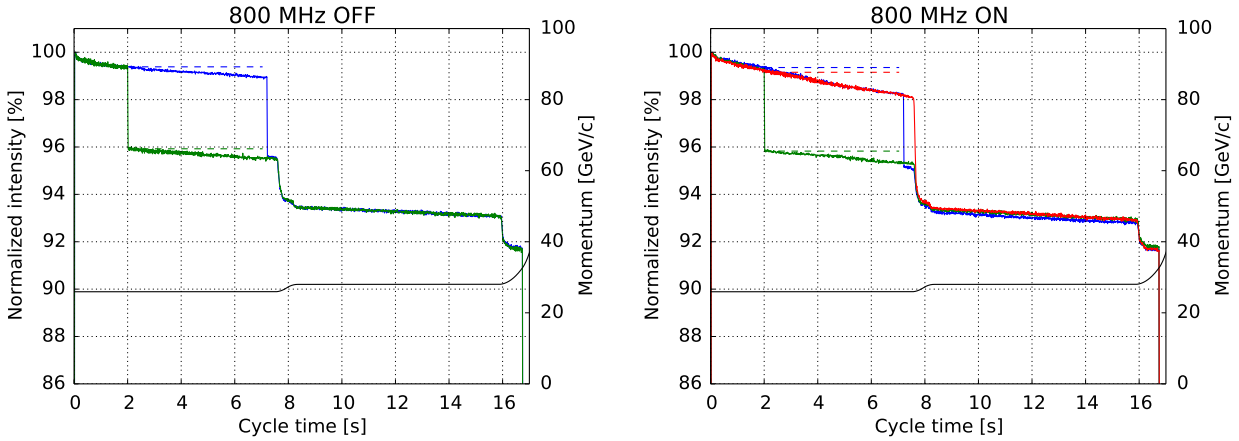

Figure 6: Intensity along the cycle when the uncaptured beam is cleaned with the MKQV tune kicker at 2 s or at 7.2 s for the case with 800 MHz OFF (left) and ON (right).

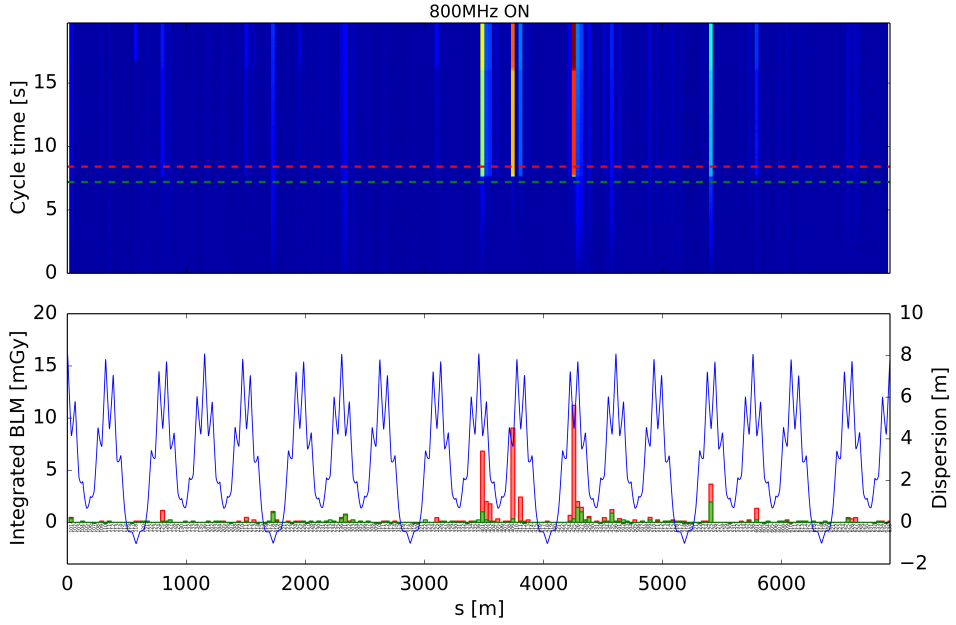

Figure 7: Losses around the SPS circumference as a function of time (top graph, color code indicates increasing losses from blue to red) and for two moments in the cycle (bottom graph, end of flat bottom in green, end of the first ramp in red).

with 800 MHz ON. As mentioned above, higher losses are observed on the flat bottom in case the 800 MHz is ON. When cleaning the uncaptured beam with the kicker at 2 s in the cycle, the losses along the remaining part of the flat bottom are very similar for both 800 MHz ON and OFF. One can therefore conclude that the uncaptured beam is lost faster with the 800 MHz RF ON, but these particles would be lost anyhow during acceleration. This is confirmed by the fact that the intensity at the end of the cycle is the same in both cases. It is interesting to note that even when cleaning the uncaptured beam a few ms before acceleration, there are still about 2% losses observed during the ramp. This could be either because not all uncaptured beam can be cleaned with the kicker (e.g. particles in the azimuthal region of the bunches are not kicked), or rather because particles close to the separatrix are lost when the bucket shape changes at the beginning of the ramp. Figure 7 shows the distribution of losses around the machine. Both the accumulated losses along the flat bottom and the losses during the first ramp are concentrated in regions with large dispersion. This is another indication that the losses are mostly related to particles with large momentum offset, such as uncaptured beam.

25 ns standard vs. 8b4e beam

To assess the possible contribution of e-cloud to the SPS flat bottom losses, the 25 ns standard beam with 72 bunches of 1.3×10^{11} p/b was compared to the 8b4e beam [10] with 48 bunches of 1.9×10^{11} p/b at injection. Like this the total

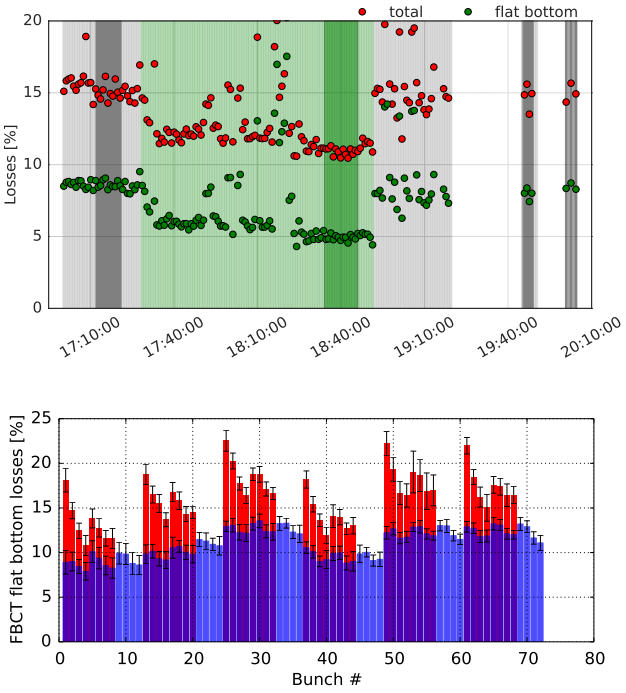

Figure 8: Losses as function of time in the MD session, where green background corresponds to times with the 25 ns standard beam and grey background to the 8b4e beam (top), and a comparison of the average bunch-by-bunch losses on the flat bottom between the two beams (bottom) taken during the time periods indicated by dark green and dark grey background.

intensity as well as the transverse emittance is the same for the two beams. In the case of the 8b4e beam the e-cloud build-up in the SPS should be negligible due to the gaps in the bunch train. Figure 8 shows the losses as function of time in the MD session (top) and a comparison of the average bunch-by-bunch losses on the flat bottom between the two beams (bottom). These average losses correspond to the periods indicated by the dark shaded time periods in the top plot (grey for 25 ns standard beam and green for the 8b4e beam). It is interesting to note that the losses along the batch show a similar pattern for the two beams, however the losses in the 8b4e beam are higher as compared to the standard beam. In addition, the losses are higher at the beginning of each group of each bunches and decrease along the sub-batches. The observations with these two beam types point towards the fact that SPS RF hardware limitations could play an important role for the losses, as discussed below.

SPS RF HARDWARE LIMITATIONS

As the review in the introduction shows, the losses along the flat bottom had been mainly discussed in the context of beam dynamics limitations and PS RF hardware limitations. In the following the SPS RF hardware limitations as far as they are relevant for losses at flat bottom and beam loading will be discussed.

200 MHz hardware

The relevant 200 MHz hardware in the SPS consists of

- four 200 MHz travelling wave structures with two structures of length $l_1 = 16$ m and two structures of length $l_2 = 20$ m
- a 1-turn delay feedback per travelling wave structure
- a feed-forward per travelling wave structure
- two longitudinal dampers, one acting through a travelling wave structure of length l_1 and one acting through a travelling wave structure of length l_2

The travelling wave structure parameters of interest here are the impedances Z_1 and Z_2. The total voltage, as seen by the beam is given by [7]

$$V = V_{\mathrm{RF}} + V_{\mathrm{b}},$$

with $V_{\mathrm{RF}} = Z_1 i_{\mathrm{g}}$ and $V_{\mathrm{b}} = Z_2 i_{\mathrm{b}}$. With

$$Z_1 \propto \frac{\sin \tau/2}{\tau/2}\, l,$$

$$Z_2 \propto -\left[\left(\frac{\sin \tau/2}{\tau/2}\right)^2 - j2\frac{\tau - \sin \tau}{\tau^2}\right] l^2$$

and

$$\tau = \frac{l}{v_{\mathrm{g}}}(\omega - \omega_0).$$

Here l is interaction length, v_{g} is the group velocity given as $v_{\mathrm{g}}/c = 0.0946$ and ω_0 the angular cavity centre frequency.

The main characteristics of the travelling wave structures is that the impedances Z_1 and Z_2 are completely different as function of frequency as illustrated in Fig. 9. This means that the beam induced voltage at certain frequencies cannot be properly compensated.

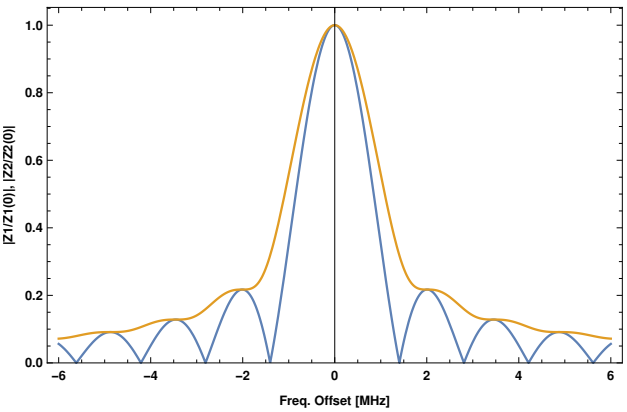

Figure 9: blue: $|Z_1(f)/Z_1(0)|$, yellow: $|Z_2(f)/Z_2(0)|$ for the case of a 5-section travelling wave structure.

To compensate the beam induced voltage in the travelling wave structures there are three elements: a polar loop, a 1-turn-delay feedback and a feed-forward. The amplitude and

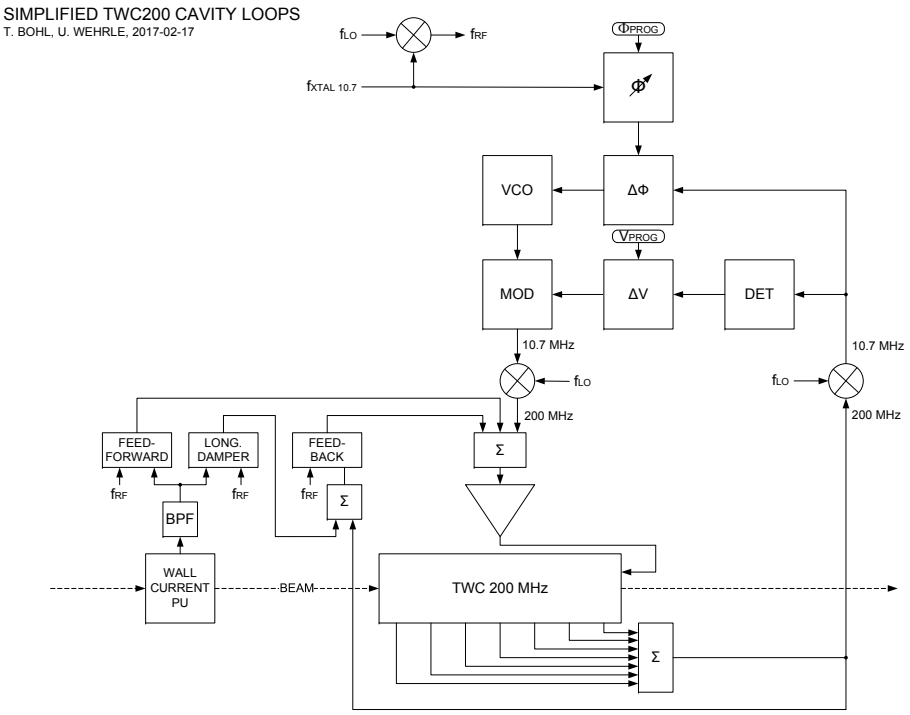

Figure 10: Simplified block diagram of cavity loops.

the phase of the voltage in the travelling wave structure is measured by a polar loop and regulated at a 1 ms time scale (bandwidth of about 1 kHz). This is the case since the SPS went into operation. Already at the beginning of the 1980s it had been realised that an impedance reduction was required to allow the acceleration of the proton fixed target beam at that time. To overcome the gain limitation of a feedback loop due to its delay, the 1-turn-delay feedback had been put into operation [8]. While the beam current component at f_{RF} is taken into account by the polar loop, the 1-turn-delay feedback takes care of the f_{rev} sidebands of f_{RF} within a bandwidth of several MHz [9]. In order to further improve the impedance reduction from about 20 dB to 26 dB, an additional feed-forward [9] was put into operation. Here the beam current is measured using a wall current monitor and the voltage required for optimal beam loading compensation is calculated by the digital feed-forward electronics and applied to the travelling wave structure.

All three devices discussed compensate the beam induced voltage in the travelling wave structures. Their performance is, however, limited by the available RF power. Another limitations is due to the difference of Z_1 and Z_2. It means in time domain that while the step response of Z_1 is linear it is parabolic for Z_2, the transient beam loading at the time the beam enters the travelling wave structure can be only approximately compensated. There is another limitation, mostly observed at injection. Here the beam executes quadrupole oscillations at twice the synchrotron frequency of $1/T_{\mathrm{s}}$, leading to a considerable variation of the beam induced voltage from turn to turn. The shorter T_{s} the worse the beam loading compensation will be due to the 1-turn delay. The three elements for beam loading compensation are shown in the simplified block diagram of the cavity loops, Fig. 10.

Limits of beam loading compensation

To illustrate the present limits of beam loading compensation, two examples will be discussed.

Example 1 The first example shows the power requirements of a 5-section travelling wave structure with a 25 ns beam of 72 bunches per batch at injection, $p = 26$ GeV/c and using the Q20 optics ($\gamma_{\mathrm{t}} = 17.95$). The number of charges per bunch, N_{Q}, was 1.9×10^{11}. Figure 11 shows the RF power, P, delivered to a 5-section travelling wave structure and the voltage, $V = V_{\mathrm{RF}} + V_{\mathrm{b}}$, measured in the same travelling wave structure. The values of P and V are shown on three time scales: on a ms time scale (top), on a μs time scale (centre) and on the time scale of a turn (bottom). On the ms time scale one can clearly identify the fully uncompensated beam induced voltage at injection (first turn) as expected. It is reduced to smaller values later on but it is not completely compensated. The total voltage can be off by more than 20% during the quadrupole oscillations at injection with any sign. The data show also that during the passage of the beam in the travelling wave structure, P, increases from the no-beam value of about 150 kW nearly 1 MW within a few 100 ns. The high peak power levels are at the limit of what the power amplifiers can deliver.

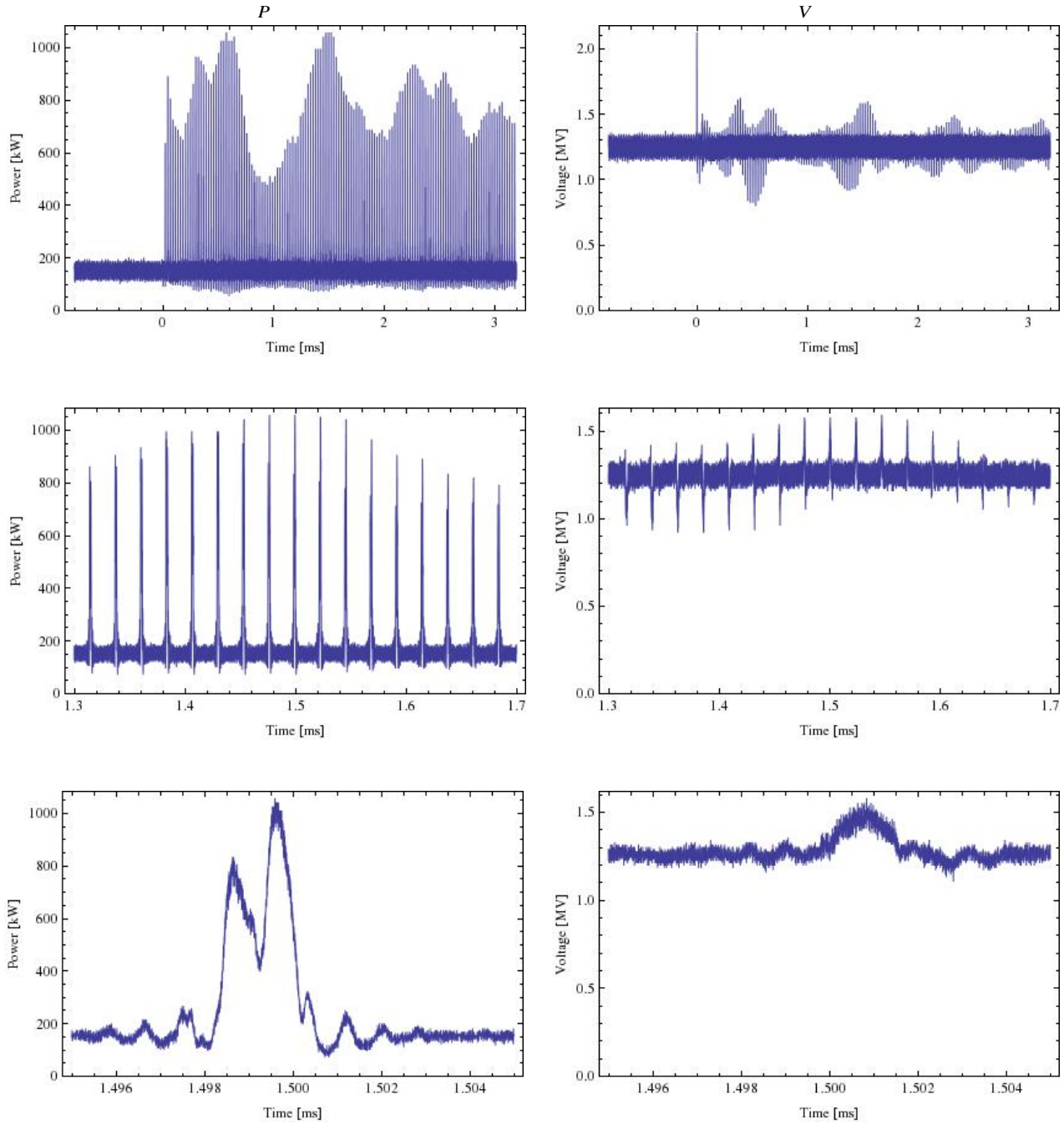

Figure 11: RF power delivered, P, and V of a 5-section travelling wave structure.

Example 2 Here a comparison of the beam loading effects at injection, $p = 26$ GeV/c, will be made using the standard 25 ns beam of 72 bunches per batch and the 8b4e beam [10] with the Q20 optics ($\gamma_t = 17.95$).

The standard 25 ns beam had the following parameters

- $N_Q = 1.3 \times 10^{11}$, $N_{Q,tot} = 9.1 \times 10^{12}$
- $l_{batch} = 1.775$ μs

The 8b4e beam had the following parameters

- $N_Q = 1.9 \times 10^{11}$, $N_{Q,tot} = 9.1 \times 10^{12}$
- $l_{batch} = 1.675$ μs

The total voltage in a 5-section travelling wave structure, V, at the first turn is shown in Fig. 12. The time of the arrival of the batch in the travelling wave structure and when it leaves the travelling wave structure can be clearly seen. Note that there is no beam loading compensation on the first turn. The power required for the beam loading compensation during the first 2 ms is shown in Fig. 13 (top). It is significantly higher for the case of the 8b4e beam. With a perfect beam loading compensation the voltage in the travelling wave structure should be constant whether the beam is

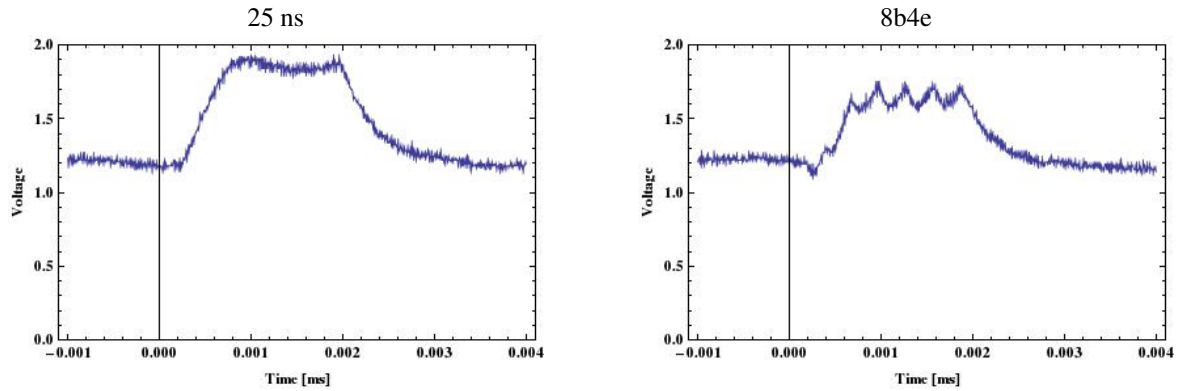

Figure 12: V at the first turn (scale: MV) for the two beams.

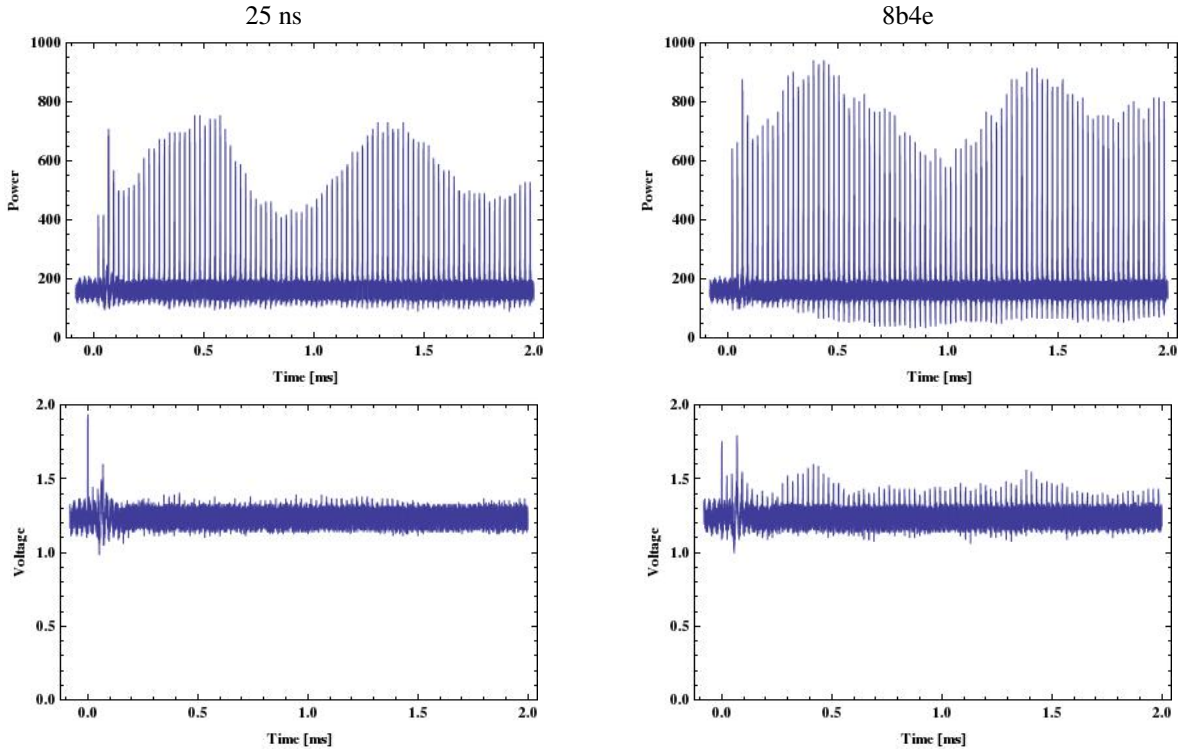

Figure 13: At the top the RF power delivered to the travelling wave structure during the first 2 ms (scale: kW) and on the bottom V during the first 2 ms (scale: MV) for the two beams.

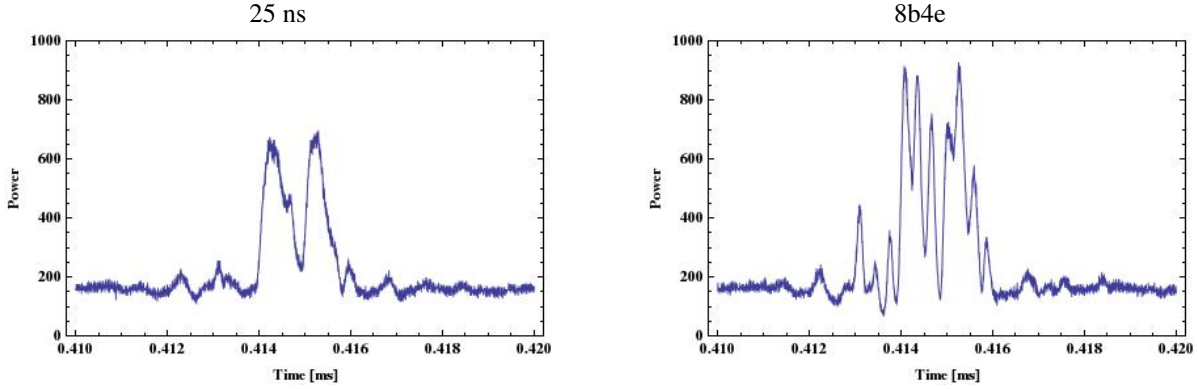

Figure 14: RF power delivered to the travelling wave structure at about 400 μs after injection (scale: kW) for the two beams.

inside the structure or not. Figure 13 (bottom) shows that this is not the case. In the case of the 25 ns beam the beam loading compensation is good after about 10 turns (25 μs). In the case of the 8b4e beam a residual error exists still after 2 ms.

A look at the power demand at about 400 μs after injection shows that the temporal structure is very different for the two beams, Fig. 14. This difference is related to the different time structures of the two beams. The frequent gaps of 8b4e require a larger bandwidth for beam loading compensation than it is necessary for the continuous beam of 72 bunches.

Longitudinal dampers

With respect to the losses at flat bottom, it is not only the beam loading in the travelling wave structures which plays a role. The two longitudinal dampers acting through the travelling structures #1 and #3 measure the bunch by bunch phase and damp longitudinal coupled bunch instabilities of low order (limited by the bandwidth of the travelling wave structures), see Fig. 10. In addition they provide the injection damping for the second and following injections of the beam as the phase loop measures only the first injected batch. Apart from the bandwidth limitation, there is another one. The longitudinal dampers had been designed for typical values of the synchrotron frequency for the Q26 optics. In the case of the Q20 optics with typically values twice or larger the damping is not any more optimal.

800 MHz hardware

The two 800 MHz travelling wave structures are now equipped with a new beam control and with a 1-turn delay feedback. The beam loading amplitude is reduced by about 26 dB and the phase variation due to beam loading is reduced to about 1° at 800 MHz. With the presently available beams there are no known limitations related to beam loading.

With respect to losses at flat bottom it had been observed that the loss rate depended on whether the 800 MHz RF system had been in use or not (see previous section). This seems to be the only point which needs to be investigated further.

Impact of LLRF settings on losses

From the above description of the SPS RF hardware it becomes clear that a global optimization of all LLRF settings requires careful measurements and multi-parametric scans. On the other hand, it can be easily tested what happens if one of the systems is switched OFF. This was done as shown in Fig. 15. For this study the 25 ns standard beam with 72 bunches of 1.33×10^{11} p/b with a bunch length of 4.1 ns at injection was used and the 800 MHz RF system was ON. The graph shows the total losses until reaching the 28 GeV/c plateau. Switching the longitudinal damper OFF had no impact on the losses, only when increasing the gain above certain levels was driving the beam unstable resulting in enhanced losses. This means that the damper is indeed not very effective in the Q20 optics as expected from the hardware limitations explained above. The biggest impact

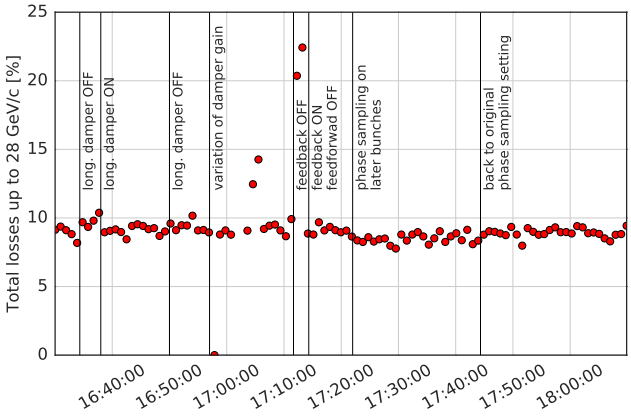

Figure 15: Losses from injection to the start of the intermediate plateau at 28 GeV/c as function of time in the MD session. The vertical bars indicate the changes in the RF settings as indicated by the labels.

on losses was observed when the 1-turn delay feedback was switched OFF, which increased the losses from 10% to more than 20%. Switching only the feed-forward OFF had no effect. This is not really expected and needs to be further studied in future MD sessions. Changing the phase loop sampling from the usual position in the beginning of the train towards the center of the batch did not change the losses.

Outlook

The hardware limitations which have been discussed will be overcome after the Long Shutdown 2. The 200 MHz 5-section travelling wave structures will be shortened and there will be only 3-section and 4-section long structures, optimal for the envisaged future beam currents. There will be two more travelling wave structures installed together with new RF power plants which will deliver higher power levels than the present ones. There will be new cavity controllers for the 200 MHz travelling wave structures with a polar loop around the RF power amplifiers, improved 1-turn delay feedback and feed-forward. In addition there will also be new longitudinal dampers which will not be limited to a particular synchrotron frequency.

In how far the beam dynamics limitations mentioned in the first part of the paper will be overcome remains to be seen.

SUMMARY AND CONCLUSIONS

Losses on the flat bottom and injection of LHC beams into the SPS are still an issue for reaching the ambitious intensity targets for the HL-LHC era. A part of the losses can clearly be attributed to capture losses due to the peculiar shape of the longitudinal distribution after the bunch rotation in the SPS, which is required at the transfer from the PS 40 MHz to the SPS 200 MHz RF structure. However, additional losses are observed on the SPS flat bottom and during the ramp. These losses seem to increase with the bunch intensity and may

not necessarily be directly related to electron cloud effects, as a comparison of the 25 ns beam with the 8b4e has shown. Instead the discussed SPS RF hardware limitations could play an important role, which however should be mitigated with the RF upgrade as part of the LIU project.

REFERENCES

[1] P. Baudrenghien, T. Bohl, T. Linnecar, E. Shaposhnikova, "Raising intensity of the LHC beam in the SPS. Longitudinal plane", SL-Note-2000-044 MD, July 2000.

[2] T. Linnecar, T. Bohl, E. Shaposhnikova and J. Tückmantel, "Capture Losses Caused by Intensity Effects in the CERN SPS", HIGH INTENSITY AND HIGH BRIGHTNESS HADRON BEAMS: 33rd ICFA Advanced Beam Dynamics Workshop on High Intensity and High Brightness Hadron Beams. AIP Conf. Proc. 773, pp. 345-349, 2004.

[3] G. Arduini, "Status & performance of the LHC (proton) Injector Complex", LHC Machine Advisory Committee, 2006-12-07.

[4] H. Timko *et al.*, "Longitudinal beam loss studies of the CERN PS-TO-SPS transfer". ICFA Workshop HB2012, China, September 2012.

[5] "LHC Injectors Upgrade Technical Design Report, Volume 1: Protons", EDMS 1451384, CERN, Geneva, Switzerland (2014).

[6] H. Bartosik, G. Arduini and Y. Papaphilippou, "Optics considerations for lowering transition energy in the SPS", IPAC11 (2011) and references therein.

[7] G. Dôme, "The SPS acceleration system travelling wave drift tube structure for the CERN SPS", CERN, Geneva, CERN-SPS/ARF/77-11, May, 1977.

[8] D. Boussard and G. Lambert, "Reduction of the apparent impedance of wide band accelerating cavities by RF feedback", IEEE Transactions on Nuclear Science, Vol. NS-30, No. 4, August 1983.

[9] P. Baudrenghien and G. Lambert, "Reducing the impedance of the travelling wave cavities. Feed-forward and one turn delay feed-back", Proc. of 10th Workshop on LEP-SPS Performance, Chamonix, France, January 2000.

[10] H. Damerau *et al.*, "LIU: Exploring alternative ideas", Review of LHC and Injector Upgrade Plans Workshop (RLIUP), 29-31 October 2013, Centre de Convention, Archamps.